BRAIN. Broad Research in Artificial Intelligence and Neuroscience
e-ISSN: 2067-3957 | p-ISSN: 2068-0473
Covered in: Web of Science (ESCI); EBSCO; JERIH PLUS (hkdir.no); IndexCopernicus; Google Scholar; SHERPA/RoMEO; ArticleReach Direct; WorldCat; CrossRef; Peeref; Bridge of Knowledge (mostwiedzy.pl); abcdindex.com; Editage; Ingenta Connect Publication; OALib; scite.ai; Scholar9; Scientific and Technical Information Portal; FID Move; ADVANCED SCIENCES INDEX (European Science Evaluation Center, neredataltics.org); ivySCI; exaly.com; Journal Selector Tool (letpub.com); Citefactor.org; fatcat!; ZDB catalogue; Catalogue SUDOC (abes.fr); OpenAlex; Wikidata; The ISSN Portal; Socolar; KVK-Volltitel (kit.edu)
2024, Volume 15, Issue 4, pages: 87-103.
Submitted: August 7th, 2024 | *Accepted for publication:* November 19th, 2024

A Hybrid Approach for CT-MR Brain Image Denoising Using PSO-Optimised Non-Local Means and Wiener Filtering

Preena Prasad
Department of Electronics and Communication Engineering, Karunya Institute of Technology and Sciences, Coimbatore, India.
Department of Electronics and Communication Engineering, SAINTGITS College of Engineering Kottayam, India.
preenabasil2014@gmail.com
https://orcid.org/0009-0007-7505-4395

Valer Niminet
Faculty of Science, Vasile Alecsandri University of Bacau, Romania.
valern@ub.ro
https://orcid.org/0009-0002-0098-8066

Anitha J.
Department of Electronics and Communication Engineering SAINTGITS College of Engineering Kottayam, India.
anithaj@karunya.edu

Abstract: *Noise in CT-MR brain images poses a critical challenge, significantly impacting diagnostic accuracy as well as clinical decision-making. Current medical image-denoising techniques struggle to effectively remove noise while preserving crucial image features. The hybrid technique's potential that combines complementary denoising algorithms is highlighted by the limitations of these approaches. This paper develops & evaluates a denoising method that combines the strengths of Particle Swarm optimised, Non-Local Means (NLM) & Wiener filtering. The proposed approach effectively denoises by leveraging non-local self-similarity in brain images. Particle Swarm Optimisation algorithm is employed to fine-tune the smoothing parameter of NLM denoising, ensuring optimal performance, while the Wiener filter helps to address the trade-off between noise reduction as well as edge preservation. The proposed denoising technique outperforms the traditional methods including median, gaussian, NLM, and wiener filter in terms of peak signal-to-noise ratio (PSNR), image quality index (IQI), mean square error (MSE), and structural similarity index (SSIM).*

Keywords: *Medical image denoising; Non local means denoising; hybrid denoising; Particle Swarm Optimization; Peak signal to noise ratio; Weiner filter.*

How to cite: Prasad, P., Niminet, V., & J., A.. (2024). A hybrid approach for CT-MR brain image denoising using PSO-optimized non-local means and Wiener filtering. *BRAIN. Broad Research in Artificial Intelligence and Neuroscience, 15*(4), 87-103. https://doi.org/10.70594/brain/15.4/7

1. Introduction

Medical image denoising is essential for improvement in the quality and accuracy of brain scanning especially in the Magnetic Resonance Imaging modality since noise is very destructive in diagnosis and intervention. It has been identified that noise, and artifacts in computed tomography and magnetic resonance imaging brain images can hide underlying anatomical structures, and pathological characteristics and even bring variability in the diagnosis of medical data. In (Goyal et al., 2018) and (Sagheer & George, 2020) Denoising techniques play an important role in enhancing the Signal-to-noise ratio, minimising image distortions, and retaining important features for use in neurology diagnosis and management. Better clinical diagnosis of CT and MR brain images can be achieved if advanced denoising techniques are applied, which leads to improved accuracy of clinical procedures and outcomes of patients.

Though Gaussian and median filtering are regularly used approaches for noise removal in medical images, these approaches have shortcomings in erasing significant structural features (Annavarapu & Borra, 2020; Chauhan & Choi, 2018; Li, 2023). Based on certain topographies Gaussian filtering may lead to the introduction of unfriendly see-through while median filtering has lesser performance especially when dealing with complex noise (Isa et al., 2015). Hence need to use a high level of denoising to help in improving contrast signal to noise as well as minimise artifacts in order to realise good details that are crucial in the diagnosis and follow-up of diseases.

Similarly, promising results have been shown with dictionary learning techniques, such as Learned Simultaneous Sparse Coding, for denoising CT and MR brain images. These methods (Tong et al., 2016) learn an overcomplete dictionary of noisy image data and then use sparse coding to obtain sparse image representations from noisy image data and separate these representations from their residue or residual noise. An advantage of these approaches is that they adapt to a particular image content so that noise is removed and detail preserved better. However, the computational complexity of dictionary learning can be higher compared to other denoising methods. Additionally, Sparse and Low-Rank Matrix Decomposition methods have demonstrated the ability to separate noise from underlying image structure (Lamare, 2015). These techniques model image as a combination of low-rank components, depicting a clean image, and sparse components, depicting noise. The key benefit is their robustness to different noise types, but the selection of appropriate regularization parameters can be challenging.

Wiener filtering is a linear, frequency domain approach that aims to minimise MSE between original and denoised images. However, it has limitations in preserving underlying image structure, as it can introduce artifacts and lose fine details (Hillery & Chin, 1991). In contrast, non-local denoising methods, such as NLM, can better preserve important details and structures by exploiting the self-similarity of image patches, without relying on specific noise and signal models. The ability of NLM denoising to remove noise while preserving fine detail makes it suitable to perform such a simple pixel replacement as denoising input using NLM operation effectively (Kazemi et al., 2016) (Buades, Coll & Morel, 2005).

Recently, hybrid denoising algorithms have gained popularity due to their capability to leverage the relative strengths of different methods to yield better-performing results. (Karnaukhov et al., 2020) Hybrid denoising algorithms that combine complementary approaches (block matching as well as 3D filtering with k-Singular Value Decomposition) have been demonstrated to show potential for Gaussian noise removal applied to polarization images. (Abubakar et al., 2020) Our results demonstrate that, by combining different denoising strategies, synergistic integration results in a better noise reduction with more preserved important features and details important in accurate medical analysis and interpretation. This suggests that the exploration of new combinations of denoising techniques can provide insight into ways that challenges of medical image processing can be addressed to improve the reliability of clinical decision-making.

Although wide research efforts have been made to improve medical image denoising, use of optimization-based techniques has been widely explored to achieve this goal (Wu et al., 2022).

These methods use advanced optimisation algorithms like PSO as well as ACO for fine-tuning parameters of different denoising filters. The ability to guide algorithms more suitably to specific characteristics and noise profiles of medical imaging modalities (for example CT and MRI) is afforded by this. In denoising brain images, PSO has been integrated with NLM filtering (Kim & Lee, 2023), combined with ACO as well as Wiener filtering (Martıin-Fernández et al., 2006). The use of optimisation-based techniques along with strengths of underlying filtering methods and advanced optimization algorithms (Dodamani & Danti, 2023) (Kushwaha & Singh, 2019) results in efficient preservation of critical medical image features as well as quality and reliability of denoised images for clinical decision-making being greatly improved.

Medical image denoising has been addressed by employing deep learning-based methods: (Bhatnagar & Jain, 2013) (Chauhan & Choi, 2018), (Parthiban & Subramanian, 2006) and (Rai et al., 2021). Convolution Neural Networks and Generative Adversarial Networks have shown remarkable performance in learning all sorts of effective noise reduction strategies from big, diverse medical image datasets (Izadi et al., 2022). Deep learning excels in learning complex, non-linear relationships between noisy inputs and clearer images, surpassing traditional denoising techniques (Chauhan & Choi, 2018) (Parthiban & Subramanian, 2006) (Rai et al., 2021). Denoising using CNN and noise-raised thresholding was implemented by Diwakar et.al., (2023). However, drawbacks of this method include over-interpretation of processed images, the need for large training data, and high computational complexity, which might pose insufficient practical implementation in real-time clinical workflows. (Pandey et al., 2024) performed the skin cancer classification, but the denoising of the image was done using NLM. The non-local means denoising algorithm is effective but its performance strongly depends on its parameters including patch, window size, and smoothing parameters (Prasad, Anitha & Biji, 2024).

In this work, we suggested a hybrid denoising method that consists of particle swarm-optimised NLM followed by Wiener filtering. The hybrid approach combines the advantages of two methods to denoise CT and MR brain images efficiently. The performance of the proposed method is exhaustively tested by established metrics like PSNR, SSIM, MSE, and IQI (Ndajah et al., 2010) to confirm denoised images meet the accuracy required for medical diagnosis and decision. The key steps of the proposed hybrid denoising technique are given below:

1. PSO Optimization of the h parameter of NLM: The h parameter of the NLM algorithm is optimised for increasing denoising efficacy using Particle Swarm Optimization.
2. Wiener Filtering: The image obtained after PSO NLM denoising is further noise reduced using a Wiener filter applied to particle swarm optimised NLM-denoised images.

An evaluation of the proposed hybrid denoising method is done on a wide CT as well as MR brain image dataset and in contrast to other state-of-the-art denoising techniques. Results demonstrate that hybrid approaches preserve critical medical image features, and achieve better quality and reliability of denoised images for clinical decision-making. The remaining paper is structured in the following pattern: section 2 describes materials and proposed methodology. In section 3 we present experimental results of denoised images and discussion. The conclusion of the work and future direction are mentioned in section 4.

2. Materials and Methods

2.1. Problem

For accurate diagnosis, medical imaging imposes the need to achieve satisfactory noise removal and detail preservation. The non-local means denoising algorithm is effective but its performance strongly depends on its parameters. So there is a need for optimising these parameters. Further improvement is needed to increase image quality.

To address this issue, in this work, we focused on improving the NLM performance by finding the optimal value for h. Optimisation of a smoothing parameter of NLM with an objective function of maximising PSNR is done by employing the particle swarm method. Thereby the output is further enhanced using the Weiner filter.

2.2. Methodology

This section presents a comprehensive explanation and analysis of proposed denoising methods. To denoise CT and MR brain images efficiently, we propose a hybrid denoising method (PSONLMW) which combines Particle Swarm Optimization enhanced NLM with Wiener filtering. PSO optimises NLM parameters, and subsequent Wiener filtering further refines denoised output.

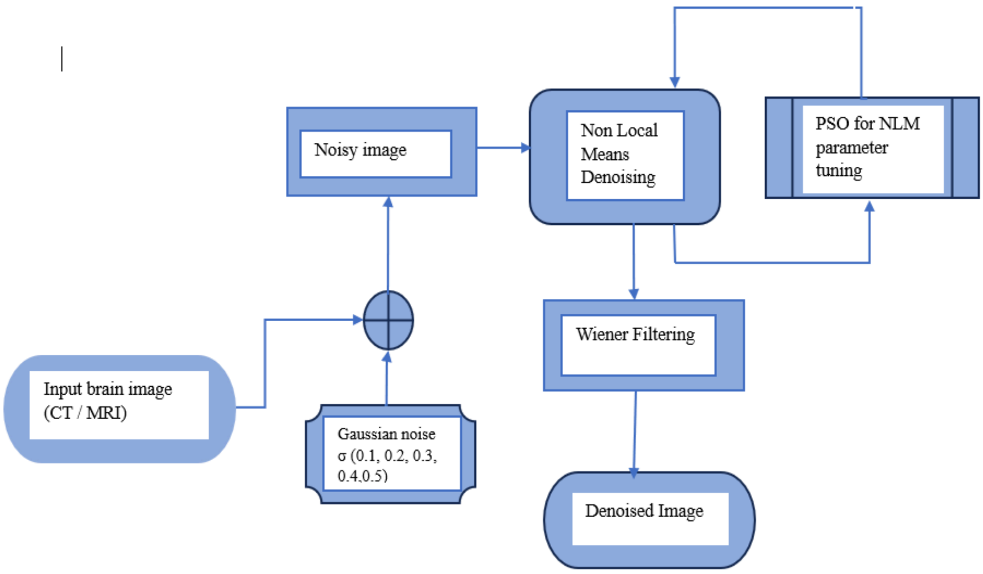

(a)

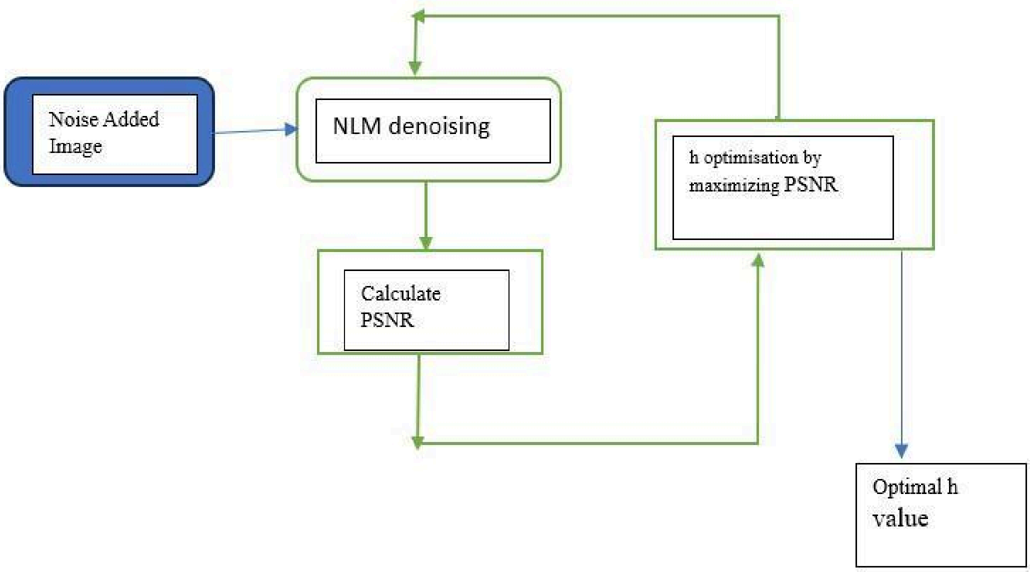

(b)

Figure 1(a). Block diagram of proposed denoising approach (PSONLMW) (b) PSONLM

The conceptual block diagram of the proposed denoising approach (PSONLMW) has been demonstrated in Figure (1a). The block diagram of the optimisation process PSONLM is included in Figure (1b). The process starts with an input image containing noise that needs to be removed. A noisy image is obtained by adding the desired noise level to a clean MR or CT image. Gaussian noise with S.D. (σ) of 0.1,0.2,0.3,0.4, and 0.5 was incorporated into the original images. Here the input image is divided into small overlapping patches (here are 3). Each patch represents a local neighborhood of pixels. After that, a search window of size larger than the patch is selected (here are 11) for finding similar patches in the region. Following it occurs the Similarity Search. Once similar patches are identified, weights are computed for each patch based on their similarity to the target patch. More similar patches receive higher weights. The weighted average of pixel values in similar patches is computed, giving more weight to more similar patches. This process effectively reduces noise while preserving the underlying image structure. Denoised pixel values from all patches are aggregated to form the final denoised image. The h parameter of NLM denoising is optimised using particle swarm optimization with the objective function of maximising PSNR.

The output of the h parameter optimised NLM filter is fed to the Wiener filter for further denoising. Incorporating the Wiener filter after PSO-optimised NLM filtering enhances the image-denoising process by addressing residual noise that the NLM algorithm might miss. NLM filter, particularly when optimised with PSO, effectively removes noise by averaging similar pixel patches based on a smoothing parameter ‘h’. However, NLM may still leave behind subtle, low-level noise, especially in regions where pixel similarities are weaker, and noise artifacts can persist. A Wiener filter is then applied to capture this residual noise by adapting to the local statistics of the denoised image. This second stage of filtering provides additional smoothing specifically tailored to areas with higher residual variance. Wiener filter reduces MSE between original and filtered images, thus refining edges and preserving structural details missed by NLM alone. PSNR is enhanced by further reducing noise power in the image while SSIM is improved by refining structural and luminance consistency. Performance evaluation is done to evaluate the quality of denoised images using performance matrices such as PSNR, SSIM, MSE, and IQI.

2.3. Non-Local Means (NLM) Denoising

A popular denoising technique, Non Local Means (NLM) is effective at preserving image details while reducing noise. NLM replaces each pixel intensity I(x) of a noisy image I with a weighted average of intensities from other pixels, where weights are based on neighbouring patches’ similarity. The amount of smoothing h has a great impact on the amount of noise reduction and detail preservation. Smoothing is stronger with a larger h, but fine details may be blurred; a smaller h does not remove enough noise. $I_{NLM}(x)$ at location x is calculated as NLM denoised pixel as given in equation (1),

$$I_{NLM}(x) = \frac{1}{C(x)} \sum_{y\in\Omega} I(y) \cdot exp(- \frac{(\|I(N_x)-I(N_y)\|^2}{h^2}) \tag{1}$$

where $C(x)$ is a normalization factor, $N_x \; and \; N_y$ are patches around pixels x and y, h controls level of filtering. Optimising h is essential for achieving high-quality denoised images.

2.4. Particle Swarm Optimisation (PSO) for Parameter Optimisation

A population-based optimization technique based on swarms of birds or schools of fish observed in nature is the underlying principle of PSO. In this study particle swarm optimization is used to find the optimal value of the smoothing parameter of the NLM filter with best PSNR to get better image quality. Each particle in the swarm is a candidate ‘h’ value and going after finding the best h that gives this best PSNR is the objective of the swarm. We had specifically used this technique for optimising smoothing parameters. In the PSO process, we initialised a swarm of particles with random ‘h’ values from a predefined range of [h_{min}, h_{max}]. Each particle owns a position (candidate h) and a velocity. Each particle’s position and velocity are updated iteratively according to individual, and collective experience. For each particle ‘i’ the updated equation is given in equation (2).

$$v_i^{(t+1)} = w \,.v_i^{(t)} + c_1 \,.r_1 \,.(p_i^{best} - x_i^{(t)} + c_2 \,.r_2 .(g_i^{best} - x_i^{(t)}) \tag{2}$$

where w represents inertia weight, $v_i^{(t)}$ is the velocity of the particle 'i' at iteration 't'. c_1 and c_2 represents cognitive and social coefficients, r_1 and r_2 are random numbers between 0 and 1, p_i^{best} is particle's personal best position, g_i^{best} is global best position obtained by swarm. Position update is given as in (3)

$$x_i^{(t+1)} = x_i^{(t)} + v_i^{(t+1)} \quad (3)$$

The new position $x_i^{(t+1)}$ is constrained within [h_{min}, h_{max}]. Each particle calculates PSNR after NLM denoising with its current h value and updates, p_i^{best} and g_i^{best} if the resulting PSNR exceeds previous values. At each iteration, the PSO algorithm evaluates denoising performance in terms of PSNR, SSIM, and MSE between denoised and original images. PSNR is used as the primary objective to be maximised, while SSIM and MSE serve as additional quality metrics. Upon convergence, the optimal h value identified by PSO yields the highest PSNR, indicating optimal noise reduction and detail preservation.

2.5. Wiener Filtering for Residual Noise Suppression

After optimising NLM parameters using PSO and applying an NLM filter, residual noise may still exist. Wiener filter is employed as a post-processing step to further reduce this residual noise by adapting to the local statistics of the image. Wiener filter in the spatial domain can be applied as in (4)

$$\hat{I}(i,j) = I(i,j) + \frac{\sigma_I^2}{\sigma_N^2}\left(I(i,j) - \bar{I}\right) \quad (4)$$

where $\hat{I}(i,j)$ is denoised pixel intensity, σ_I^2 and σ_N^2 are variances of image and noise, respectively. $\bar{I}$ is the local mean intensity around the pixel. Applying Wiener filter post-PSO-optimised NLM filtering captures residual noise not fully removed by NLM, further improving PSNR and SSIM by refining output.

2.6. Gray wolf Optimisation

The metahuristic algorithm based upon the social hierarchy and hunting startegies of Gray Wolf is called Gray Wolf optimisation. The optimisation process based on the hierarchy of leadership in Wolf pack is implemented in GWO with Alpha, beta, delta and omega wolves corrresponding to the candidate solution. Optimisation is done through simulating the wolve's hunting behavior.Here we had optimised the h parameter using GWO algorithm and compared with PSONLM keeping the comparison as runtime.

2.7. Materials

Experimentation is performed using a diverse dataset of computed tomography (CT) and Magnetic resonance image (MRI). CT images and MR images for the brain are taken for experimentation from publicly available dataset from Kaggle. MR images are taken from the publicly available benchmark dataset "Br35H:: Brain Tumor detection 2020". It has 3060 images of brain MR images. CT images are taken from the publicly available dataset from Kaggle named "Computed Tomography (CT) of the Brain". This dataset has 259 CT images of the brain. This dataset comprises 7,023 MRI scans of the human brain, categorised into four classes: glioma, meningioma, no tumor, and pituitary. In this paper, two MR images and two CT images are used to represent the result of experimentation. An experiment was done using the software MATLAB R2022b on a 12th Gen Intel(R) Core (TM) i7-12700 operating at 2100MHz, X64-based PC.

2.8. Performance Metrics

Mean Square Error (MSE): A commonly utilised statistic for evaluating denoising is MSE. The squared difference is computed as the average squared difference between a pixel in the original image and the same pixel in the denoised image. The better the denoising performance, the lower the MSE values. It is calculated using the equation (5).

$$\text{MSE}=\frac{1}{MN}\sum_{i=}\sum_{.1j=1}^{nN}(\bar{I}\,(i,j)-I_{denoised}\,(i,j))^2 \qquad (5)$$

Here, $\bar{I}\,(i,j)$ is the original pixel value, and $I_{denoised}\,(i,j)$ is the corresponding denoised pixel value.

Structural Similarity Index (SSIM): SSIM measure quantifies the similarity between 2 images on the basis of brightness, structure, and contrast attributes. This metric is often utilised for denoising evaluation because of its assessment of perceptual image quality. The range of SSIM values is 0-1, with elevated values suggesting superior denoising efficacy. SSIM is responsive to image content and may not be suitable for any type of image.

Peak Signal-to-Noise Ratio(PSNR): PSNR is among the most frequently utilised metrics for assessing denoising methods. It quantifies the ratio of the signal's maximum potential value to the noise level. This is computed as specified in equation(6).

$$\text{PSNR}=10\log10((\text{MAX}_I)^2/\text{MSE}) \qquad (6)$$

Here MAX_I represents the maximum possible pixel value and MSE denotes the mean squared error between the denoised image and the original one. Increased PSNR values signify superior denoising efficacy.

Image Quality Index (IQI): It is a metric to determine image quality on the basis of a comparison of an image with a reference or original image. Structural, luminance, and contrast information of the original image are evaluated by IQI on how well it is retained after processing.

3. Results & Discussion

We have compared the proposed method PSONLMW's performance with other existing denoising methods including Median, Gaussian, Wiener, NLM, and also with the output of Particle Swarm Optimised Non-Local Means (PSONLM). An evaluation was done using brain MR and CT images with Gaussian noise of different intensities. Results show the robustness of each filter by comparing metrics including PSNR, SSIM, MSE, and IQI.

Table 1. Performance comparison of different filters with Gaussian noise of σ=0.1

Image	Filter	PSNR	SSIM	MSE	IQI
Brain MR image1	Median Filter	27.69	0.4839	0.0017	0.9509
	Gaussian Filter	31.08	0.6888	0.0008	0.9766
	Wiener Filter	31.38	0.7384	0.0007	0.9781
	Non-Local Means Denoising filter	34.79	0.9262	0.0003	0.9897
	Particle Swarm Optimised NLM	35.56	0.9185	0.0003	0.9914
	PSONLMW	**35.95**	**0.9363**	0.0003	**0.9922**
Brain MR image2	Median Filter	29.01	0.4816	0.0013	0.9697
	Gaussian Filter	28.10	0.3939	0.0016	0.9537
	Wiener Filter	27.20	0.3507	0.0019	0.9456
	Non-Local Means Denoising filter	26.05	0.3725	0.0025	0.9277

	Particle Swarm Optimised NLM	28.89	0.3357	0.0018	0.9610
	PSONLMW	**29.06**	0.4410	0.0012	**0.9622**
Brain CT image1	Median Filter	28.23	0.4933	0.0015	0.9921
	Gaussian Filter	25.31	0.3330	0.0029	0.9809
	Wiener Filter	26.23	0.3361	0.0024	0.9838
	Non-Local Means Denoising filter	20.14	0.1995	0.0097	0.9452
	Particle Swarm Optimised NLM	27.15	0.3401	0.0019	0.9865
	PSONLMW	**27.63**	0.3514	0.0017	**0.9875**
Brain CT image2	Median Filter	28.24	0.4920	0.0015	0.9916
	Gaussian Filter	25.10	0.3250	0.0031	0.9781
	Wiener Filter	26.21	0.3286	0.0024	0.9818
	Non-Local Means Denoising filter	19.82	0.1907	0.0104	0.9369
	Particle Swarm Optimised NLM	27.10	0.3303	0.0020	0.9848
	PSONLMW	**27.61**	0.3425	0.0017	**0.9859**

Four images included in this paper are named Brain MR image1, Brain MR image2, Brain CT image1, and Brain CT image2. Original images were added with Gaussian noise of S.D. (σ) of 0.1, 0.2, 0.3, 0.4, and 0.5. Quantitative analysis results of various denoising filters and algorithms are presented in Tables 1, 2, and 3. Denoised images produced for various filtering techniques are depicted in Figures 2, 3, 4, 5, 6, 7, 8, 9, and 10.

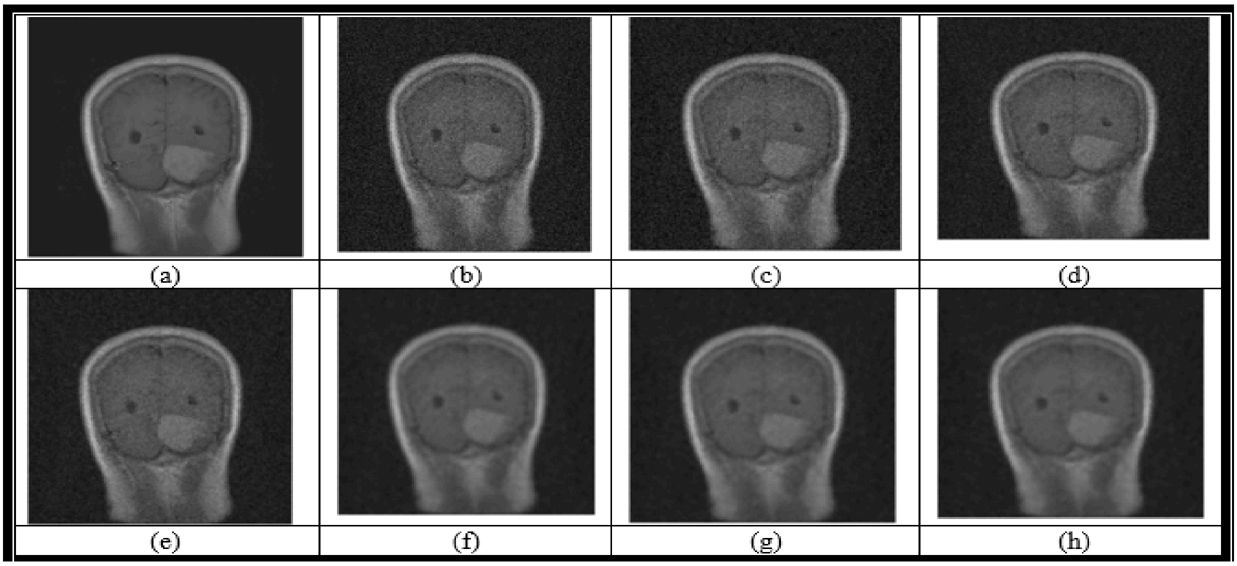

Figure 2. Denoised image output of the Brain MR image1 with σ=0.1 (a) Original image (b) Noisy image (c) Median Filter (d) Gaussian Filter (e) Wiener Filter (f) Non-Local Means filter (g) Particle Swarm Optimised Non-Local Means filter (h) Particle Swarm Optimised Non-Local Means Wiener filter.

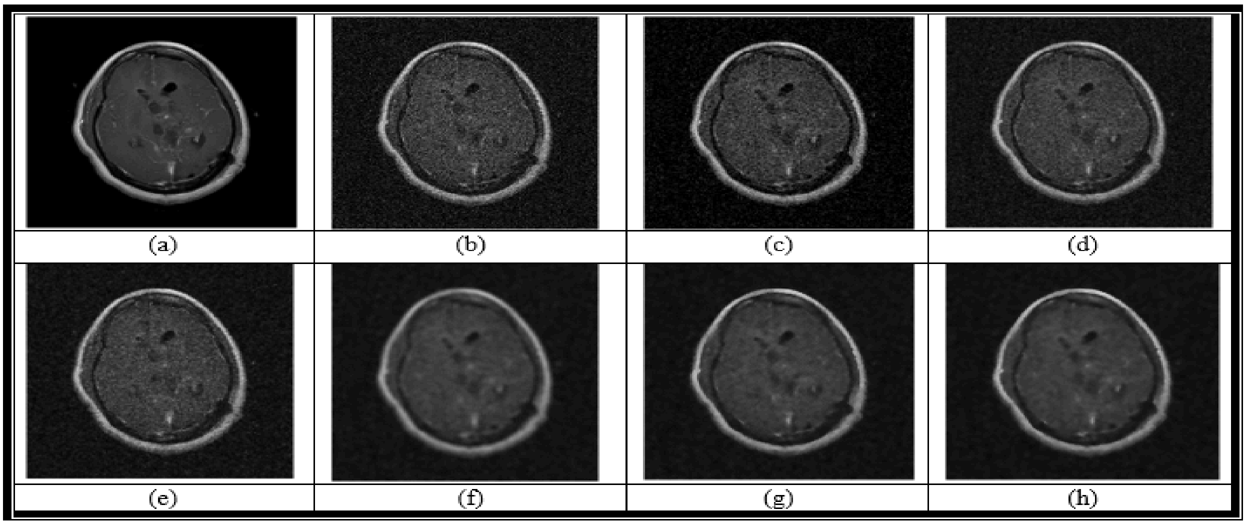

Figure 3. Denoised image output of the Brain MR image2 with σ=0.1 (a) Original image (b) Noisy image (c) Median Filter (d) Gaussian Filter (e) Wiener Filter (f) Non-Local Means filter (g) Particle Swarm Optimised Non-Local Means filter (h) Particle Swarm Optimised Non-Local Means Wiener filter.

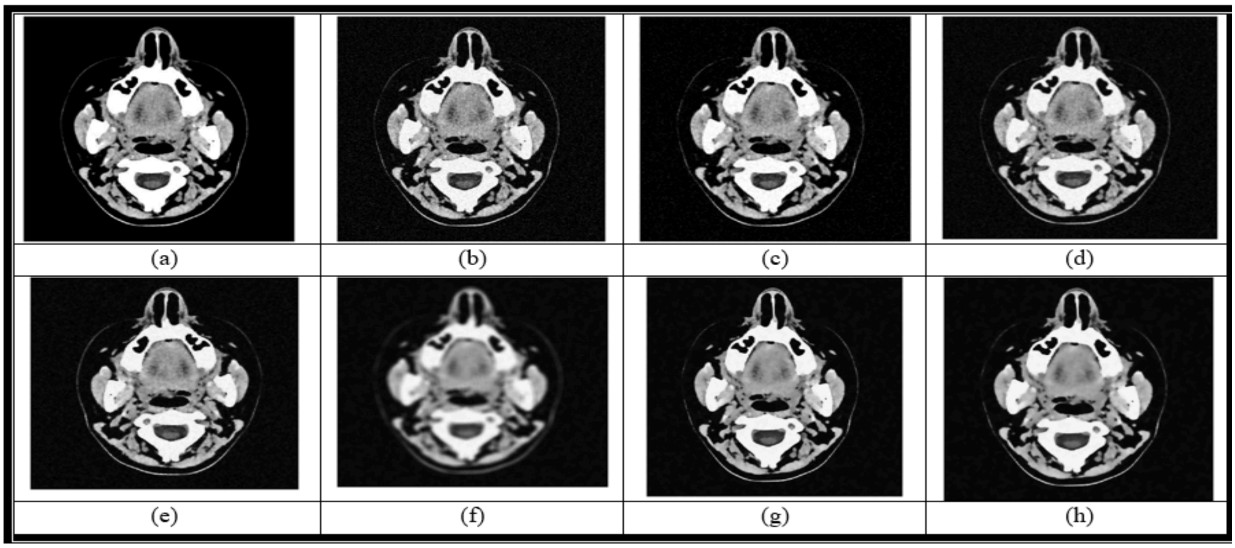

Figure 4. Denoised image output of the Brain CT image1 with σ=0.1 (a) Original image (b) Noisy image (c) Median Filter (d) Gaussian Filter (e) Wiener Filter (f) Non-Local Means filter (g) Particle Swarm Optimised Non-Local Means filter (h) Particle Swarm Optimised Non-Local Means Wiener filter.

The proposed method's performance is compared to traditional methods for denoising a noisy image which is obtained by incorporating Gaussian noise with S.D. (σ)0.1 to a set of clean images and is shown in Table 1. Performance in terms of Brain MR image1 PSNR, SSIM, and IQI are 35.95, 0.9363, and 0.9922 respectively. Results showed a PSNR and SSIM of 29.06, 0.9622 for denoised Brain MR image2. PSNR and SSIM achieved for Brain CT image1 and Brain CT image2 are (27.63, 0.9875) and (27.61, 0.9859). It is also noted that the MSE obtained for PSONLMW is very low compared to all other methods. The result shows that MSE for Brain CT image1 after performing non-local means denoising is 0.0097 which is significantly reduced to 0.0017 for PSONLMW. At the same time, PSNR increased from 20.14 to 27.63.

For the sample images proposed method PSONLMW gives the largest value for denoising in terms of PSNR, SSIM, and IQI along with the smallest MSE for Gaussian noise of (σ) 0.1. Figures 2, 3, and 4 show the original, noisy, and denoised output of different filtering methods on Brain MR image1, Brain MR image2, and Brain CT image1. The original image was further added with the Gaussian noise of S.D.(σ) of 0.2,0.3,0.4, and 0.5 as well as analysed the performance. Table 2 shows the result of denoising using existing and proposed methods of noisy images obtained by incorporating Gaussian noise of standard deviations (σ) 0.2 and 0.3 to clean images. The PSNR is increased in Brain CT image1 after performing PSONLMW (when compared with traditional NLM) with a p-value of 0.0231 and MSE decreased with a p-value of .0342 for a Gaussian noise of 0.2.

Table 2. Performance comparison of different filters with Gaussian noise

Image	Filter	*σ=0.2*				*σ=0.3*			
		PSNR	SSIM	MSE	IQI	PSNR	SSIM	MSE	IQI
Brain MR image1	Median Filter	22.041	0.2194	0.00624	0.8401	18.91	0.1229	0.0128	0.7151
	Gaussian Filter	25.14	0.4263	0.0031	0.9135	21.34	0.2792	0.0074	0.8191
	Wiener Filter	25.03	0.4889	0.0031	0.9109	21.38	0.3439	0.0073	0.8197
	Non-Local Means Denoising filter	26.01	0.7634	0.0041	0.9515	24.66	0.7983	0.0034	0.9321
	Particle Swarm Optimised NLM	27.61	0.7716	0.0021	0.9616	24.72	0.6101	0.0035	0.9277
	PSONLMW	**29.95**	**0.8478**	**0.0010**	0.9720	**25.33**	**0.7353**	**0.0029**	**0.9317**
Brain MR image2	Median Filter	20.31	0.1892	0.0046	0.8929	17.78	0.1543	0.0098	0.7866
	Gaussian Filter	20.36	0.2438	0.0058	0.8450	18.86	0.1717	0.0130	0.7137
	Wiener Filter	21.61	0.2509	0.0069	0.8223	18.44	0.1313	0.0143	0.6887
	Non-Local Means Denoising filter	22.42	0.2870	0.0057	0.8396	19.46	0.2691	0.0113	0.7368
	Particle Swarm Optimised NLM	**23.39**	**0.2844**	0.0046	0.8711	19.98	**0.2627**	0.0104	0.7622
	PSONLMW	**25.70**	**0.6579**	0.0043	0.8786	20.41	**0.5232**	0.0091	0.7784
Brain CT image1	Median Filter	18.52	0.3039	0.0048	0.8742	16.92	0.2003	0.0182	0.8404
	Gaussian Filter	20.36	0.2499	0.0080	0.8946	18.29	0.2011	0.0161	0.8409
	Wiener Filter	20.70	0.1638	0.0141	0.9100	18.81	0.2502	0.0129	0.8604
	Non-Local Means Denoising filter	21.17	0.2265	0.0085	0.9325	19.01	0.0351	0.0113	0.8612
	Particle Swarm Optimised NLM	22.17	**0.2502**	0.0069	0.9333	20.12	**0.3999**	0.0124	0.9131
	PSONLMW	26.23	**0.5932**	0.0041	0.9632	25.11	**0.5992**	0.0098	0.9470
Brain CT image2	Median Filter	18.27	0.1548	0.0149	0.8976	17.84	0.1977	0.0164	0.8794
	Gaussian Filter	20.69	0.2231	0.0085	0.9367	17.52	0.1721	0.0177	0.8730
	Wiener Filter	20.87	0.2439	0.0082	0.9300	16.61	0.1405	0.0218	0.8433
	Non-Local Means Denoising filter	22.14	0.2533	0.0074	0.9316	18.81	0.2014	0.0133	0.9011
	Particle Swarm Optimised NLM	**24.08**	**0.4585**	0.0062	0.9461	19.02	0.2223	0.0125	0.9041
	PSONLMW	**27.08**	**0.6585**	0.0029	0.9598	22.07	0.6205	0.0098	0.9426

In particular, when the noise level rises to 0.2, the performance of denoising filters has a significant effect on image quality, where results are distinct across different filters. For example, in Brain MR Image1, with increased noise, a PSNR of 29.95, SSIM of 0.8478, MSE of 0.0010, and IQI of 0.9720 are held by PSONLMW filter with a strong performance. It can be seen however that the PSONLMW filter can deal with higher noise levels without losing structural details.

On the other hand, the median filter exhibits a drastic fall off in performance, with a PSNR of 22.041, SSIM of 0.2194, MSE of 0.00624, and IQI of 0.8401, thus indicating its incapability to remove noise as noise level escalates. Gaussian filter and wiener filter also demonstrate moderate declines, with the Gaussian filter outputting a PSNR of 25.14, SSIM of 0.4263, MSE of 0.0031, IQI of 0.9135 and wiener filter outputting a PSNR of 25.03, SSIM of 0.4889, MSE of 0.0031, IQI of 0.9109. Figure 5 shows the original, noisy as well as denoised output of different filtering methods on Brain CT image1 for Gaussian noise of 0.3.

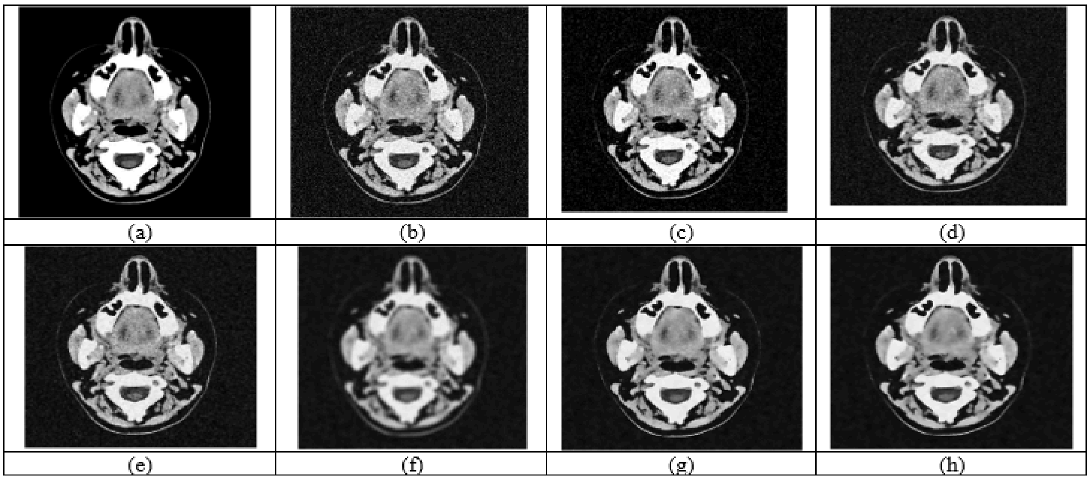

Figure 5. Denoised image output of the Brain CT image1 with σ=0.3 (a)Original image (b)Noisy image (c)Median Filter (d)Gaussian Filter (e)Wiener Filter (f)Non-Local Means filter (g)Particle Swarm Optimised Non-Local Means filter (h)Particle Swarm Optimised Non-Local Means Wiener filter.

These results confirm that traditional filters do provide some improvement, although the robust performance of these filters is not guaranteed in the presence of increasing noise levels as compared to advanced filters like PSONLMW. For the NLM denoising filter, there is also a noticeable decrease in performance, with a PSNR of 26.01, SSIM of 0.7634, MSE of 0.0041, and IQI of 0.9515, demonstrating that while usable, it is far worse compared to PSONLMW denoiser under high noise conditions. As a result, an increased noise of 0.2 justifies the advantage of employing the proposed denoising method PSONLMW, which surpasses standard filters. Figure 6 and Figure 7 show the original, noisy, and denoised output of different filtering methods on Brain MR image Gaussian noise of 0.2 and 0.3 respectively.

Table 3 shows the result of denoising for Gaussian noise of σ 0.4 and 0.5. Performance comparison of different filters applied to images with Gaussian noise levels of σ=0.4 and σ=0.5 reveals clear trends regarding the effectiveness of each filter in denoising images. PSONLMW filter gives the highest PSNR values of 22.01 (σ=0.4) and 19.89 (σ=0.5), showing superior image quality preservation compared to other filters for Brain MR image1.

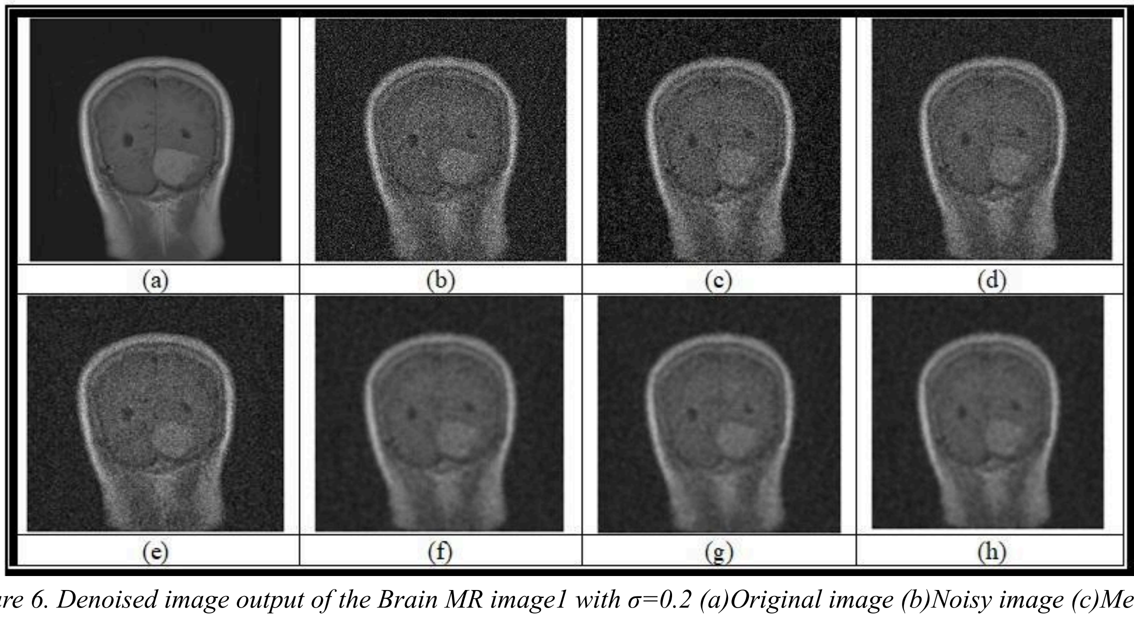

Figure 6. Denoised image output of the Brain MR image1 with σ=0.2 (a)Original image (b)Noisy image (c)Median Filter (d)Gaussian Filter (e)Wiener Filter (f)Non-Local Means filter (g)Particle Swarm Optimised Non-Local Means filter (h)Particle Swarm Optimised Non-Local Means Wiener filter.

In Brain CT image1, the PSONLMW filter also yields the highest PSNR of 18.73 at σ=0.4, and 16.98 at σ=0.5, again outperforming other methods, particularly for σ=0.4, where improvement is more notable. For Brain CT image2, PSONLMW achieves the highest PSNR of 17.71 (σ=0.4) and 15.99 (σ=0.5), continuing its superior performance in preserving image quality. Figures 8 and 9 show the original, noisy, and denoised output of different filtering methods on Brain MR image 1 for Gaussian noise of 0.4 and 0.5 respectively. Figure 10 shows the result of denoising of CT image2 for a noise of standard deviation 0.2, 0.3, and 0.4 respectively.

In the case of SSIM, PSONLMW consistently delivers the highest SSIM across all images and noise levels. For example, in Brain MR image1, SSIM values obtained are 0.6539 (σ=0.4) and 0.6515 (σ=0.5), indicating higher structural similarity preservation. PSONLMW also provides the highest SSIM in Brain CT image1 (0.5675 at σ=0.4 and 0.5362 at σ=0.5), suggesting its effectiveness in maintaining image structure despite increasing noise levels. Noise reduction capability is better for low MSE values. PSONLMW filter demonstrates the lowest MSE values, such as 0.0063 (σ=0.4) and 0.0103 (σ=0.5) for Brain MR image1 and 0.0169 (σ=0.4) and 0.0102 (σ=0.5) for Brain CT image1. These results indicate that PSONLMW is most effective in minimising errors between original and denoised images. Efficacy in preserving image quality and structural details is proven by higher values of IQI. For Brain MR image1, IQI values are 0.8743 (σ=0.4) and 0.8159 (σ=0.5), while for Brain CT image1, IQI values are 0.9090 (σ=0.4) and 0.8665 (σ=0.5). In Brain CT image2, PSONLMW achieves 0.9022 (σ=0.4) and 0.8577 (σ=0.5), indicating that the filter is highly effective in maintaining overall image quality under noisy conditions.

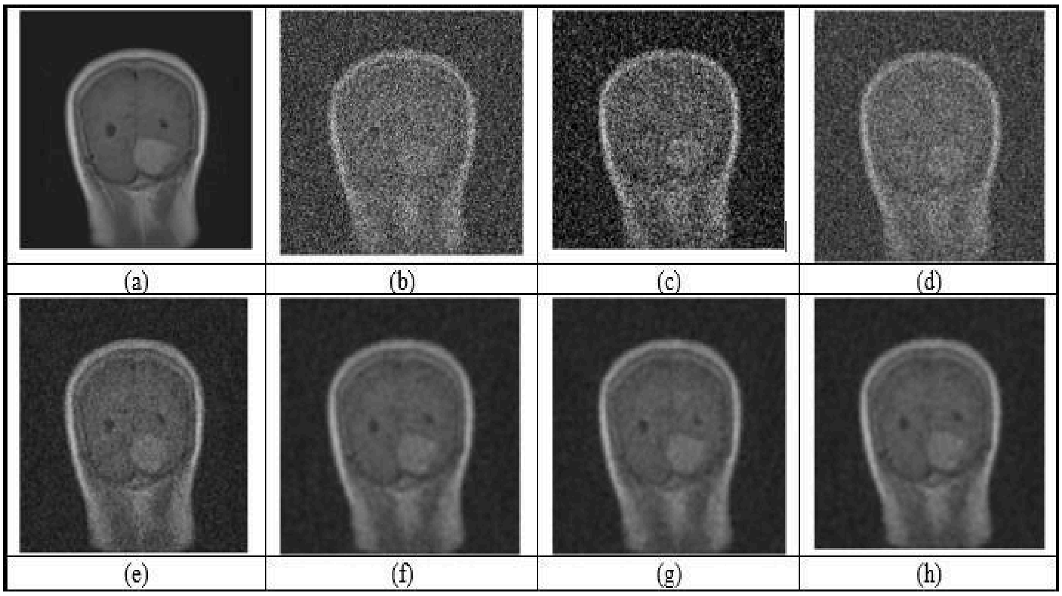

Figure 7. Denoised image output of the Brain MR image1 with σ=0.3 (a - h) Original image, Noisy image, Median Filter, Gaussian Filter, Wiener Filter, Non-Local Means filter, Particle Swarm Optimised Non-Local Means filter, Particle Swarm Optimised Non-Local Means Wiener filter.

Table 3. Performance comparison of different filters with Gaussian noise

Image	Filter	*σ=0.4*					*σ=0.5*			
		PSNR	SSIM	MSE	IQI		PSNR	SSIM	MSE	IQI
Brain MR image1	Median Filter	**16.70**	0.0797	0.0213	0.5905		15.04	0.0562	0.0312	0.4855
	Gaussian Filter	18.67	0.1995	0.0136	0.7086		16.91	0.1528	0.0304	0.6076
	Wiener Filter	19.04	0.2610	0.0125	0.7306		17.39	0.2170	0.0204	0.6506
	Non-Local Means Denoising filter	21.22	0.6178	0.0075	0.8690		18.01	0.4521	0.0201	0.7507
	Particle Swarm Optimised NLM	21.39	0.4733	0.0074	0.8636		18.89	0.4997	0.0154	0.7518
	PSONLMW	**22.01**	**0.6539**	**0.0063**	**0.8743**		**19.89**	**0.6515**	**0.0103**	0.8159
Brain MR image2	Median Filter	16.02	0.1027	0.0169	0.4692		14.06	0.0751	0.0253	0.5609
	Gaussian Filter	16.37	0.1304	0.0231	0.5834		14.64	0.1028	0.0344	0.4778
	Wiener Filter	17.02	0.1035	0.0239	0.5709		14.71	0.0911	0.0338	0.4819
	Non-Local Means Denoising filter	17.10	0.2424	0.0195	0.6314		15.41	0.2195	0.0288	0.5453
	Particle Swarm Optimised NLM	18.56	0.4045	0.0350	0.6493		15.84	0.0608	0.0310	0.5591
	PSONLMW	**21.03**	0.6002	0.0161	0.6735		**17.20**	**0.5943**	0.0194	0.5975
Brain CT image1	Median Filter	15.63	0.1667	0.0274	0.8206		13.93	0.1244	0.0404	0.7436
	Gaussian Filter	15.43	0.1420	0.0286	0.8142		13.93	0.1286	0.0405	0.7320
	Wiener Filter	15.20	0.1378	0.0302	0.7975		14.21	0.1426	0.0398	0.7469
	Non-Local Means Denoising filter	16.47	0.1428	0.0232	0.8489		14.00	0.1422	0.0378	0.7469
	Particle Swarm Optimised NLM	16.73	0.1964	0.0212	0.8551		14.80	0.4645	0.1771	0.7825
	PSONLMW	**18.73**	0.5675	0.0169	0.9090		**16.98**	**0.5362**	0.0102	0.8665
Brain CT image2	Median Filter	15.04	0.1289	0.0313	0.7762		13.89	0.1254	0.0408	0.7265
	Gaussian Filter	15.39	0.141	0.0289	0.7996		13.78	0.1190	0.0418	0.7077
	Wiener Filter	15.56	0.1657	0.0278	0.8051		13.93	0.1397	0.0405	0.7283
	Non-Local Means Denoising filter	16.23	0.1391	0.0240	0.8362		14.25	0.3681	0.0762	0.7666
	Particle Swarm Optimised NLM	16.51	0.3895	0.0216	0.8415		14.97	0.4314	0.0318	0.7739
	PSONLMW	**17.71**	0.5690	0.0169	0.9022		**15.99**	0.5381	0.0252	0.8577

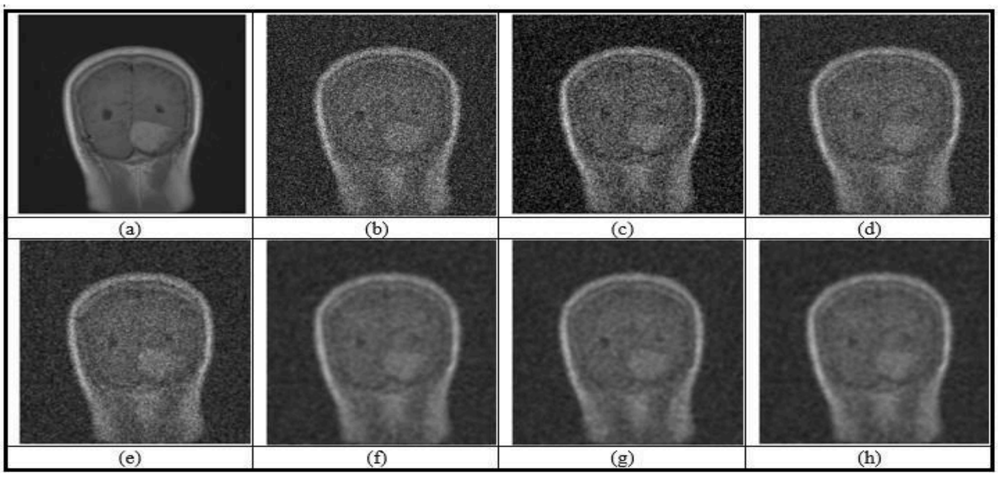

Figure 8. Denoised image output of the Brain MR image1 with σ=0.4 (a)Original image (b)Noisy image (c)Median Filter (d)Gaussian Filter (e)Wiener Filter (f)Non-Local Means filter (g)Particle Swarm Optimised Non-Local Means filter (h)Particle Swarm Optimised Non-Local Means Wiener filter.

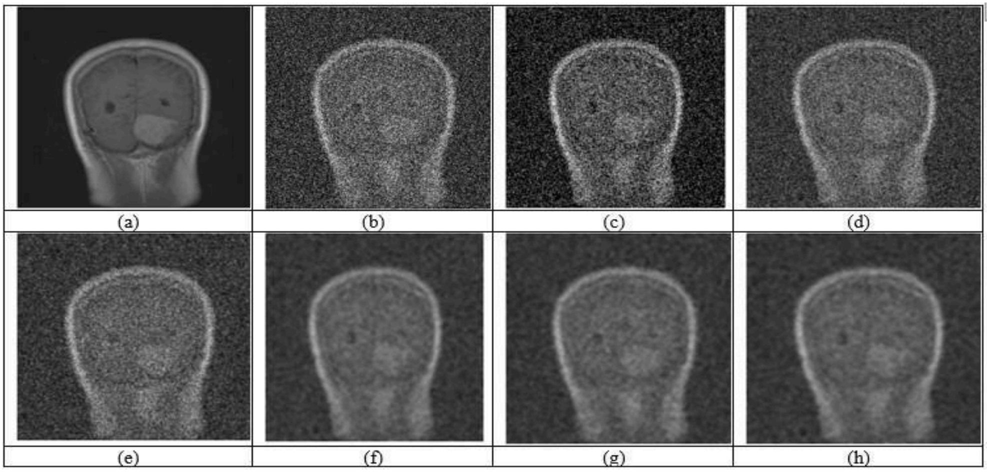

Figure 9. Denoised image output of the Brain MR image1 with σ=0.5 (a)Original image (b)Noisy image (c)Median Filter (d)Gaussian Filter (e)Wiener Filter (f)Non-Local Means filter (g)Particle Swarm Optimised Non-Local Means filter (h)Particle Swarm Optimised Non-Local Means Wiener filter.

Table 4. Comparison of performance with gray wolf optimisation and particle swarm optimisation

Image *σ=0.1*	Filter	PSNR	SSIM	MSE	Run time
Brain MR image1	Particle Swarm Optimised NLM	35.56	0.9185	0.0002	120.73s
	Gray Wolf Optimised NLM	34.52	0.8909	0.0003	350.29s
Brain MR image2	Particle Swarm Optimised NLM	28.89	0.3357	0.0018	120.7s
	Gray Wolf Optimised NLM	26.90	0.2513	0.0013	392.10s

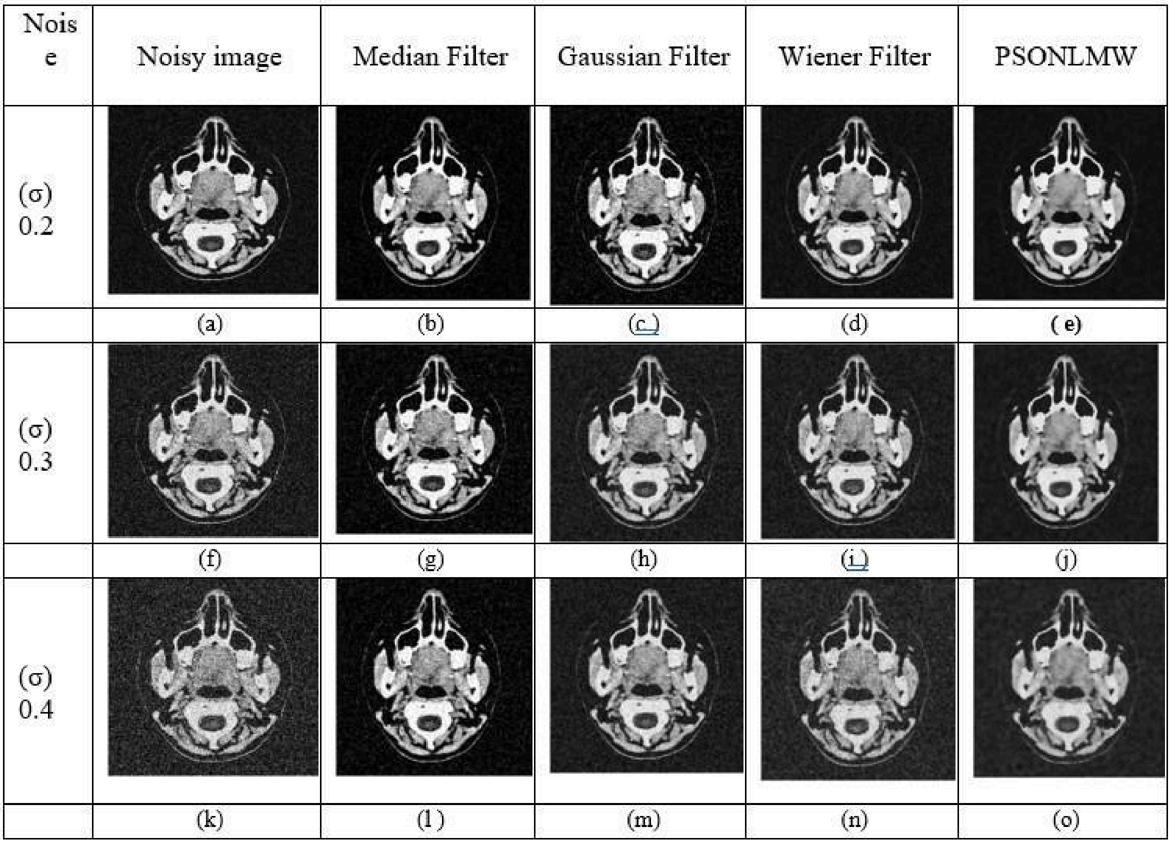

Figure 10. Denoised image output of the Brain CT image2 with σ=0.2 (a - e) with σ=0.3 (f – j) with σ=0.4 (k – o) Noisy image, Median Filter, Gaussian Filter, Wiener Filter, Particle Swarm Optimised Non-Local Means Wiener filter.

Table 4 shows a comparison of performance with gray wolf optimisation and particle swarm optimization. We had done the experimentation for all the images. The result of denoising Brain MR image1 and Brain MR image2 added with noise of standard deviation of 0.1 are tabulated. It is found that the result obtained by using PSO has a better run time (120.73s and 350.29s for PSO, GWO respectively for Brain MR image1) leading to improved computational efficiency and lower computational cost.

Effectiveness across all noise levels: PSONLMW consistently denoised medical images in all noise levels with superior PSNR and SSIM than other methods, which indicates that it is a robust and adaptable denoiser. For moderate noise, NLM and PSONLM did quite well, while traditional filters including Median and Gaussian did not perform as well under high noise. These results highlight the advantages of incorporating particle swarm optimization with NLM filtering and wiener filtering (PSONLMW) for denoising applications in medical imaging. Results show that the PSONLMW filter outperformed traditional filters in preserving both structural details and overall image quality, consistently improving PSNR, SSIM, and IQI across both MR and CT images.

The performance gap between PSONLMW and other methods was most evident in high-noise conditions, where the optimised approach maintained comparatively high-quality metrics, thereby suggesting its suitability for noisy environments often encountered in practical medical imaging scenarios. It has been observed that the proposed method PSONLMW can provide desired noise reduction, without a large loss of image quality, for applications where noise intensity is variable or high. Optimised approaches are demonstrated to preserve structural integrity and visual quality across all noise intensities in this study, thus, PSONLMW contributes to the field of medical image denoising and may serve as a reliable tool for better diagnostic accuracy in medical image applications.

4. Conclusion

In this work, Particle Swarm Optimised NLM along with Wiener filtering have been presented for denoising MR and CT brain images. Results of experimentation substantiated the fact that the proposed hybrid denoising technique (PSONLMW), denoising based on Particle Swarm optimised NLM and Wiener filter accurately removes noise from CT and MR Brain images. PSO-based optimization gave better results of h-parameter optimisation, especially in terms of run time. The hybrid method entails the benefits of two methods; which accelerate the keeping of vital features of medical images while eradicating noise, and resultant images are very well suited for precise diagnosis of diseases. The first major merit of the suggested hybrid denoising technique is the increasing ability to regulate the parameter of NLM in denoising of CT and MR brain images, as well as the Wiener filter, minimises the mean square error between original and filtered images, thus refining edges and preserving structural details missed by NLM alone. Experimental outcomes demonstrate that the proposed method PSONLMW outperforms other traditional approaches. This work can be extended to include exploring the application of the proposed method to other medical imaging modalities, including ultrasound, and PET scans, to expand its utility in diverse clinical settings. Additionally, other optimization algorithms can be explored to further improve the denoising capabilities of a hybrid approach.

References

Abubakar, A., Zhao, X., Takruri, M., Bastaki, E., & Bermak, A. (2020). A hybrid denoising algorithm of BM3D and KSVD for Gaussian noise in DoFP polarization images. *IEEE Access*, *8*, 57451–57459. https://doi.org/10.1109/ACCESS.2020.2982535

Annavarapu, A., & Borra, S. (2020, September 17). Development of magnetic resonance image de-noising methodologies: A comprehensive overview of the state-of-the-art. *Elsevier BV*, *18*, 100138. https://doi.org/10.1109/RBME.2021.3055556

Bhatnagar, S., & Jain, R. (2013, December 1). Different denoising techniques for medical images in wavelet domain. *Journal of Signal and Image Processing*, *1*, 325–329. https://doi.org/10.1109/ICSPCom.2013.6719806

Buades, A., Coll, B., & Morel, J. (2005, July 27). A non-local algorithm for image denoising. *Proceedings of the IEEE Conference on Computer Vision and Pattern Recognition (CVPR)*, 60–65. https://doi.org/10.1109/cvpr.2005.38

Chauhan, N., & Choi, B. (2018, September 30). Performance analysis of denoising algorithms for human brain image. *Journal of Biomedical Imaging*, *18*(3), 175–181. https://doi.org/10.5391/IJFIS.2018.18.3.175

Diwakar, M., Pandey, N. K., Singh, R., Sisodia, D., Arya, C., Singh, P., & Chakraborty, C. (2023). Low-dose COVID-19 CT image denoising using CNN and its method noise thresholding. *Current Medical Imaging*, *19*(2), 182–193. https://doi.org/10.2174/1573405618666220404162241

Dodamani, P. S., & Danti, A. (2023, June 30). Grey Wolf Optimization guided non-local means denoising for localizing and extracting bone regions from X-ray images. *Oriental Scientific Publishing Company*, *16*(2), 935–946. https://doi.org/10.13005/bpj/2676

Goyal, B., Dogra, A., Agrawal, S., & Sohi, B. (2018, September 13). Noise issues prevailing in various types of medical images. *Oriental Scientific Publishing Company*, *11*(3), 1227–1237. https://doi.org/10.13005/bpj/1484

Hillery, A., & Chin, R. (1991, January 1). Iterative Wiener filters for image restoration. *IEEE Transactions on Signal Processing*, *39*(8), 1892–1899. https://doi.org/10.1109/78.91161

Isa, I. S., Sulaiman, S. N., Mustapha, M., & Darus, S. (2015, January 1). Evaluating denoising performances of fundamental filters for T2-weighted MRI images. *Elsevier BV*, *60*, 760–768. https://doi.org/10.1016/j.procs.2015.08.231

Izadi, S., Sutton, D., & Hamarneh, G. (2022, November 15). Image denoising in the deep learning era. *Journal of Imaging Science and Technology*, *56*(7), 5929–5974. https://doi.org/10.1007/s10462-022-10305-2

Karnaukhov, V. E., Krylov, A. S., Ding, Y., & Farias, M. C. Q. (2020, August 21). Hybrid method for biomedical image Poisson denoising. *Journal of Biomedical Imaging*, *45*(8), 215–221. https://doi.org/10.1145/3417519.3417553

Kazemi, M., Mohammadi, P., Sadeghi, P. S., & Menhaj, M. B. (2016, January 1). A non-local means approach for Gaussian noise removal from images using a modified weighting kernel. *Cornell University Library*. https://doi.org/10.48550/arXiv.1612.01006

Kim, K., & Lee, Y. (2023, January 1). Optimization of search window and mask size for non-local means noise reduction algorithm in chest digital tomosynthesis. *Journal of Medical Imaging and Health Informatics*. https://doi.org/10.1007/s40042-024-01007-9

Kushwaha, S., & Singh, R. K. (2019, April 12). Optimization of the proposed hybrid denoising technique to overcome over-filtering issue. *De Gruyter*, *64*(5), 601–618. https://doi.org/10.1515/bmt-2018-0101

Lamare, R. C. D. (2015, January 1). *Low-rank signal processing: Design, algorithms for dimensionality reduction and applications*. *Cornell University*. https://doi.org/10.48550/arXiv.1508.00636

Li, S. (2023, January 1). Enhancement of the prefiltered rotationally invariant non-local PCA algorithm for MRI. *Cornell University*. https://arxiv.org/abs/2301.07389

Ndajah, P., Kikuchi, H., Yukawa, M., Watanabe, H., & Muramatsu, S. (2010, November 3). SSIM image quality metric for denoised images. *Proceedings of the International Conference on Image Processing and Computer Vision*, 53–57.

Parthiban, L., & Subramanian, R. (2006, October 30). MRI image denoising for telemedicine. *International Journal of Computer Applications*, 188–191.https://doi.org/10.1109/HEALTH.2006.246445

Pandey, A., Teja, M. S., Sahare, P., Kamble, V., Parate, M., & Hashmi, M. F. (2024). Skin cancer classification using non-local means denoising and sparse dictionary learning based CNN. *Journal of Electrical Systems and Information Technology*, *11*(1), 36. https://doi.org/10.1186/s43067-024-00162-0

Prasad, P., Anitha, J., & Biji, B. (2024, March). Performance analysis of non-local means denoising on medical images and the impact of filter parameter variation. In *2024 International Conference on Wireless Communications, Signal Processing and Networking (WiSPNET)* (pp. 1–5). IEEE.

Rai, S., Bhatt, J. S., & Patra, S. K. (2021, January 1). An unsupervised deep learning framework for medical image denoising. *Cornell University*. https://doi.org/10.48550/arXiv.2103.06575

Sagheer, S. V. M., & George, S. N. (2020, June 26). A review on medical image denoising algorithms. *Elsevier BV*, *61*, 102036. https://doi.org/10.1016/j.bspc.2020.102036

Tong, T., Caballero, J., Bhatia, K. K., & Rueckert, D. (2016, January 1). Dictionary learning for medical image denoising, reconstruction, and segmentation. In *Medical Image Computing and Computer-Assisted Intervention (MICCAI 2016)* (pp. 153–181). Springer. https://doi.org/10.1016/B978-0-12-804076-8.00006-2

Wu, M., Chen, Y., Zhu, P., & Chen, W. (2022, September 1). NLM parameter optimization for φ-OTDR signal. *Journal of Optical Communications and Networking*, *14*(9), 849–858. https://doi.org/10.1109/JLT.2022.3186830